11-2014

Nonlinear Dichroism in Back-to-Back Double Ionization of He by an Intense Elliptically Polarized Few-Cycle Extreme Ultraviolet Pulse

Jean Marcel Ngoko Djiokap
University of Nebraska-Lincoln, marcelngoko@unl.edu

N. L. Manakov
Voronezh State University, manakov@phys.vsu.ru

A. V. Meremianin
Voronezh State University, meremianin@phys.vsu.ru

S. X. Hu
University of Rochester

L. B. Madsen
Aarhus University

See next page for additional authors

Nonlinear Dichroism in Back-to-Back Double Ionization of He by an Intense Elliptically Polarized Few-Cycle Extreme Ultraviolet Pulse

J. M. Ngoko Djiokap,[1] N. L. Manakov,[2] A. V. Meremianin,[2] S. X. Hu,[3] L. B. Madsen,[4] and Anthony F. Starace[1]
[1]*Department of Physics and Astronomy, University of Nebraska, Lincoln, Nebraska 68588-0299, USA*
[2]*Department of Physics, Voronezh State University, Voronezh 394006, Russia*
[3]*Laboratory for Laser Energetics, University of Rochester, Rochester, New York 14623, USA*
[4]*Department of Physics and Astronomy, Aarhus University, DK-8000 Aarhus C, Denmark*
(Received 13 May 2014; revised manuscript received 2 October 2014; published 26 November 2014)

Control of double ionization of He by means of the polarization and carrier-envelope phase (CEP) of an intense, few-cycle extreme ultraviolet (XUV) pulse is demonstrated numerically by solving the six-dimensional two-electron, time-dependent Schrödinger equation for He interacting with an elliptically polarized XUV pulse. Guided by perturbation theory (PT), we predict the existence of a nonlinear dichroic effect ($\propto I^{3/2}$) that is sensitive to the CEP, ellipticity, peak intensity I, and temporal duration of the pulse. This dichroic effect (i.e., the difference of the two-electron angular distributions for opposite helicities of the ionizing XUV pulse) originates from interference of first- and second-order PT amplitudes, allowing one to probe and control S- and D-wave channels of the two-electron continuum. We show that the back-to-back in-plane geometry with unequal energy sharing is an ideal one for observing this dichroic effect that occurs only for an elliptically polarized, few-cycle attosecond pulse.

DOI: 10.1103/PhysRevLett.113.223002 PACS numbers: 32.80.Fb, 02.70.Dh, 02.70.Hm, 32.80.Rm

The quantum dynamics of two-electron atomic systems interacting with electromagnetic fields is a fundamental problem. It is well known that electron correlation underlies the fundamental process of single-photon double ionization of He [1]. Owing to recent advances in producing extreme ultraviolet (XUV) pulses by means of harmonic generation [2] or free-electron lasers [3–6], the nonlinear process of two-photon double ionization of He has been observed. The key role played by electron correlation in two-photon double ionization of He has subsequently been extensively investigated (see, e.g., Refs. [7–23]). All these investigations concern the case of linearly polarized XUV pulses.

Use of elliptically polarized light opens the possibility of investigating effects and target properties that are not accessible with linearly polarized pulses. For example, investigations of atomic and molecular ionization by circularly and/or elliptically polarized ultrashort pulses have revealed "counterintuitive angular shifts" in ionized electron angular distributions [24] (explained subsequently as due to a dynamical phase shift [25]), imprints of target orbital structures on photoelectron angular distributions [26,27], and the ability of a circularly polarized pulse to serve as an attoclock for timing strong field and attosecond ionization processes [28]. In these works for atoms the three-dimensional time-dependent Schrödinger equation (TDSE) is solved using the single-active-electron approximation. General formulations for single ionization of an atom [25] and double ionization of He [29] by an arbitrarily polarized, few-cycle XUV pulse using perturbation theory (PT) have been validated numerically *only* for the case of a linearly polarized pulse [29–32] owing to its axial symmetry, which reduces the numerical effort. None of these many prior numerical investigations has addressed the challenging six-dimensional problem of a two-electron system interacting with an arbitrarily polarized XUV pulse.

In this Letter we study double photoionization (DPI) of He by an intense, elliptically polarized, few-cycle attosecond XUV pulse. Our focus is the dependence of the two-electron angular distributions on the carrier-envelope phase (CEP) and the *helicity* of the pulse both by a PT analysis and by solving *ab initio* the six-dimensional TDSE for He. Owing to the large bandwidth of the few-cycle pulse, our numerical results reveal a new type of CEP-sensitive polarization asymmetry that is normally absent in single photon double ionization of He. The asymmetry is present in the two-electron angular distributions under a change of the rotation direction of the polarization of the attosecond pulse. The different angular distributions for opposite helicities of the pulse is our main finding, and we refer to this effect as "nonlinear dichroism" (ND). Its physical origin, within the framework of PT, is the interference of first-order (A_1) and second-order (A_2) transition amplitudes [cf. Fig. 1(a)]. In the absence of electron correlation, $A_1 = 0$ and ND vanishes. Moreover, ND probes electron correlation on its natural time scale since ND vanishes also for long pulses.

For the pulse parameters employed here, PT in the pulse amplitude is valid and can be employed to both guide numerical calculations and interpret their results. A key fact is that experiments with elliptically polarized pulses provide information that is in principle inaccessible to experiments with linearly polarized pulses. We parameterize the

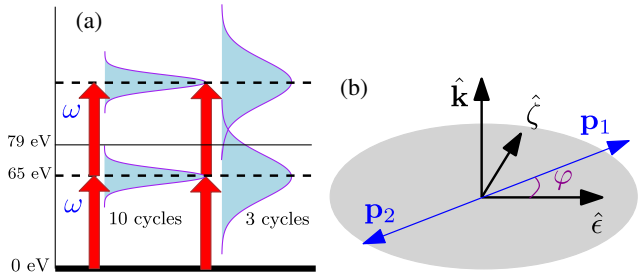

FIG. 1 (color online). (a) Sketch of two-electron energy spectra produced when He absorbs one or two photons from a single ten- or three-cycle pulse with $\omega = 65$ eV. For the three-cycle pulse, the one- and two-photon perturbation theory amplitudes (A_1 and A_2) overlap at ≈4 eV above the DPI threshold at 79 eV owing to the large pulse bandwidth. (b) The in-plane back-to-back (BTB) geometry for DPI of He with electron momenta $\mathbf{p}_1$ and $\mathbf{p}_2$ in the polarization plane orthogonal to the laser propagation direction $\hat{\mathbf{k}}$. The major and minor axes of the polarization ellipse are defined by the unit vectors $\hat{\boldsymbol{\epsilon}}$ and $\hat{\boldsymbol{\zeta}}$. The BTB angle, φ, is the angle between $\hat{\mathbf{p}}_1$ and $\hat{\boldsymbol{\epsilon}}$.

pulse polarization vector, $\mathbf{e}$, as $\mathbf{e} = (\hat{\boldsymbol{\epsilon}} + i\eta\hat{\boldsymbol{\zeta}})/\sqrt{1+\eta^2}$, where $\hat{\boldsymbol{\epsilon}}$ and $\hat{\boldsymbol{\zeta}} = \hat{\mathbf{k}} \times \hat{\boldsymbol{\epsilon}}$ indicate respectively the major and minor axes of the polarization ellipse, $\hat{\mathbf{k}}$ is the pulse propagation direction, and η is the ellipticity ($-1 \le \eta \le +1$). [Note that the circular polarization degree, ξ, of the pulse is $\xi = 2\eta/(1+\eta^2)$.] Defining the triply differential probability (TDP) for DPI by $d^3W/dEd\Omega_{\hat{\mathbf{p}}_1}d\Omega_{\hat{\mathbf{p}}_2} \equiv \mathcal{W}(\mathbf{p}_1, \mathbf{p}_2, \mathbf{e})$, where $\mathbf{p}_{1,2}$ are the electron momenta and $E = (p_1^2 + p_2^2)/2$, dynamical and phase information on the DPI process for a pulse with $\xi \neq 0$ can be gained by measuring the difference of the TDPs for pulses with the electric field $\mathbf{F}$ rotating in opposite directions, i.e., the dichroic effect [33]. We refer to this difference as the dichroism ΔW_ξ,

$$\Delta\mathcal{W}_\xi \equiv \mathcal{W}(\mathbf{p}_1, \mathbf{p}_2, \mathbf{e}) - \mathcal{W}(\mathbf{p}_1, \mathbf{p}_2, \mathbf{e}^*). \quad (1)$$

We describe the interaction of an atom in its $^1S^e$ ground state with a short pulse electric field $\mathbf{F}(t) = F_0(t)\mathrm{Re}[\mathbf{e}e^{-i(\omega t+\phi)}]$ having CEP ϕ, carrier frequency ω, and temporal envelope function $F_0(t)$. We neglect spin-orbit interactions, so that both amplitudes A_1 and A_2 are scalars independent of the quantization axis. We adopt the same PT assumptions as in Refs. [25,29]. Under these assumptions (see the Supplemental Material [34] for a discussion), the TDP equals

$$\mathcal{W}(\mathbf{p}_1, \mathbf{p}_2, \mathbf{e}) \approx \mathcal{C}[|A_1|^2 + 2\mathrm{Re}(A_1^* A_2)], \quad (2)$$

where $\mathcal{C}$ is a normalization factor. The validity of Eq. (2) is determined by comparing with TDSE calculations.

Using Eq. (2) in Eq. (1), we see that $\Delta\mathcal{W}_\xi$ is comprised of two very different parts. One of them, $\Delta\mathcal{W}_{D1}$, results from the interference of different terms in the first-order amplitude A_1; it is the analog of conventional circular dichroism in single photon double ionization of He [1,35–41] and is linear in the pulse intensity I. The second part, $\Delta\mathcal{W}_{D12}$, is due to interference of the first- and second-order amplitudes, as occurs in single electron short-pulse ionization [25]. It is a nonlinear dichroic effect since $\Delta\mathcal{W}_{D12} \propto I^{3/2}$. By choosing a geometry in which $\Delta\mathcal{W}_{D1}$ vanishes, one can thus measure the ND term $\Delta\mathcal{W}_{D12}$ directly. Such a geometry is back-to-back (BTB) emission of the two electrons [1]; cf. Fig. 1(b). For other geometries, PT indicates that the linear dichroism term $\Delta\mathcal{W}_{D1}$ is generally larger than $\Delta\mathcal{W}_{D12}$. Note that $\Delta\mathcal{W}_{D12}$ vanishes upon averaging over the CEP ϕ; it also vanishes whenever the first-order amplitude vanishes due to selection rules. In the latter case ND originates from the interference between different terms in the second-order amplitude. This higher-order dichroism, $\Delta\mathcal{W}_{D2} \propto I^2$, has the same general properties as $\Delta\mathcal{W}_{D12}$, and its role is elucidated by our numerical calculations below.

The first-order PT amplitude, A_1, for single-photon DPI to the continuum $^1P^o$-state of the ionized electron pair with energy E can be parameterized as in Ref. [29]:

$$A_1 = e^{-i\phi}[f_g(\rho)(\mathbf{p}_+ \cdot \mathbf{e}) + f_u(\rho)(\mathbf{p}_- \cdot \mathbf{e})], \quad (3)$$

where $\rho \equiv (p_1, p_2, \theta)$, θ is the mutual angle between the electron momenta, and $\mathbf{p}_\pm \equiv (\hat{\mathbf{p}}_1 \pm \hat{\mathbf{p}}_2)/2$ (cf. [34] for discussion). The Pauli exclusion principle and parity conservation require the functions $f_{g,u}$ to be symmetric and antisymmetric, i.e., $f_g(p_2, p_1, \theta) = f_g(p_1, p_2, \theta)$ and $f_u(p_2, p_1, \theta) = -f_u(p_1, p_2, \theta)$. Note that A_1 vanishes for equal energy sharing ($p_1 = p_2$) in the BTB geometry ($\hat{\mathbf{p}}_1 = -\hat{\mathbf{p}}_2$) since in that case both $f_u(\rho)$ and $\mathbf{p}_+$ vanish.

For an "in-plane geometry" (i.e., $\mathbf{p}_1$, $\mathbf{p}_2$, and $\mathbf{e}$ all lie in the polarization plane), the first-order circular dichroism, $\Delta\mathcal{W}_{D1}$, depends *only* on the degree of circular polarization ξ and is independent of both the CEP and the orientation (i.e., φ) of the polarization ellipse with respect to the electron momenta, as follows from the explicit expression for $\Delta\mathcal{W}_{D1}$ that one obtains using Eq. (3):

$$\frac{1}{\mathcal{C}}\Delta\mathcal{W}_{D1} = |A_1(\mathbf{e})|^2 - |A_1(\mathbf{e}^*)|^2 = \pm\xi\sin\theta\mathrm{Im}[f_g^* f_u]. \quad (4)$$

Here $\pm$ is the sign of the triple product $(\hat{\mathbf{k}} \cdot [\hat{\mathbf{p}}_1 \times \hat{\mathbf{p}}_2])$. Note that $\Delta\mathcal{W}_{D1}$ vanishes for the BTB geometry ($\theta = \pi$).

For a sufficiently short pulse, one- and two-photon transitions (described by the first- and second-order amplitudes, A_1 and A_2) may each doubly ionize an initial $^1S^e$ state leading to two-electron continuum states with the same energy E [cf. Fig. 1(a) for the three-cycle case]. (Note that A_2 includes both two-photon absorption and absorption and emission involving two photons.) By electric dipole selection rules, A_1 leads to electron pairs in $^1P^o$ states, while A_2 leads to $^1S^e$ and $^1D^e$ states. In contrast to $\Delta\mathcal{W}_{D1}$, the ND part of Eq. (1), $\Delta\mathcal{W}_{D12}$ [obtained within PT for unequal energy sharing and the BTB in-plane geometry,

cf. Fig. 1(b)], depends not only on ξ but also on the CEP, the orientation φ of the polarization ellipse, and on the product $\xi\ell$, where $\ell = (1-\eta^2)/(1+\eta^2)$ is the degree of linear polarization. As explained in the Supplemental Material [34], $\Delta\mathcal{W}_{D12}$ equals

$$\Delta\mathcal{W}_{D12} = \mathcal{C}\xi\sqrt{2/(\ell+1)}\sin\varphi\,\mathrm{Im}\{f_u^*[e^{-i\phi}(2h\ell - h_- \times(\ell\cos 2\varphi + 1)) + e^{i\phi}(2h' + h'_-(\ell\cos 2\varphi + 1))]\}, \quad (5)$$

where h, h_-, h', and h'_- are CEP- and η-independent dynamical parameters describing the amplitude A_2 [34]. Equation (5) shows that the ND term $\Delta\mathcal{W}_{D12}$ involves the product of the dynamical parameter f_u^* of A_1 [cf. Eq. (3)] and the dynamical h parameters [34] characterizing A_2; therefore $\Delta\mathcal{W}_{D12}$ vanishes unless the pulse bandwidth is sufficiently large that these parameters of A_1 and A_2 are nonzero at the same energy.

Unlike for linearly polarized pulses, for elliptically polarized pulses the angular momentum projection M is not conserved. This results in an "M-mixing problem" [42,43] that we treat using ideas introduced in Ref. [43] and developed further in Refs. [24,26–28,44]. We solve the six-dimensional TDSE using a finite-element discrete-variable representation and the real-space product algorithm [45] together with Wigner rotation transformations at each time step to the frame of the instantaneous electric field [24,26–28,42–44]. We calculate the TDP, $\mathcal{W}(\mathbf{p}_1,\mathbf{p}_2,\mathbf{e})$, for ionization of two electrons that share the energy $E = E_1 + E_2$ above the DPI threshold, by projecting the continuum part $\Phi_C(\boldsymbol{r}_1,\boldsymbol{r}_2,\phi,\mathbf{e})$ of the two-electron wave packet (at a time $\approx$20 a.u. after the pulse, ensuring convergence) onto field-free states, $\Psi^{(-)}_{\mathbf{p}_1,\mathbf{p}_2}(\boldsymbol{r}_1,\boldsymbol{r}_2)$, which are uncorrelated symmetrized products of two Coulomb functions for $Z = 2$ [29,46],

$$\mathcal{W}(\mathbf{p}_1,\mathbf{p}_2,\mathbf{e}) = |\langle\Psi^{(-)}_{\mathbf{p}_1,\mathbf{p}_2}(\boldsymbol{r}_1,\boldsymbol{r}_2)|\Phi_C(\boldsymbol{r}_1,\boldsymbol{r}_2,\phi,\mathbf{e})\rangle|^2. \quad (6)$$

Our calculations include 199 partial waves for four values of L: $0 \le L \le 3$, so that effects of the small third-order PT amplitude are included. We assume a pulse envelope $F_0(t) = F_0\cos^2(\pi t/T)$ with $-T/2 \le t \le T/2$, where $T \equiv n(2\pi/\omega)$ is the total pulse duration for $n = 3$ optical cycles. The temporal full width at half maximum of the pulse intensity profile is $0.364T = 1.1$ cycles, which is comparable to those of the linearly polarized, single-cycle pulses achieved experimentally [47,48]. The spectral width $\Delta\omega \simeq 1.44\omega/n$ [18] of the pulse intensity profile is 31.2 eV for $\omega = 65$ eV ($T = 190.9$ as) and our peak pulse intensity is 2 PW/cm^2. Significant interference, for $\omega = 65$ eV, occurs at energies $E \approx 4$ eV [29] above the DPI threshold energy ($\approx$79 eV) at which the PT amplitudes A_1 and A_2 are comparable [cf. Fig. 1(a)].

We present results of our numerical calculations for the BTB geometry [Fig. 1(b)] since the first-order circular dichroism $\Delta\mathcal{W}_{D1}$ vanishes [cf. Eq. (4)]. An additional virtue of the BTB scheme is that it guarantees a high accuracy of our numerical method in the XUV regime (with convergence of our results for a relatively low number of electron angular momenta) since the torque along the BTB axis is always zero [49]. All but one of the results in Figs. 2–4 are given for unequal energy sharing.

The strong CEP dependence of the TDPs $\mathcal{W}(\hat{\mathbf{p}},\mathbf{e}) \equiv \mathcal{W}(\mathbf{p}_1,\mathbf{p}_2,\mathbf{e})|_{\hat{\mathbf{p}}_2=-\hat{\mathbf{p}}_1}$ [cf. Eq. (6)] for $\xi = \pm 0.8$ are shown in Figs. 2(a)–2(d) for four CEPs. For each CEP, comparing the TDPs for $\xi \to -\xi$ (or equivalently, $\mathbf{e} \to \mathbf{e}^*$), one sees that the angular distributions, $\mathcal{W}(\hat{\mathbf{p}},\mathbf{e})$ and $\mathcal{W}(\hat{\mathbf{p}},\mathbf{e}^*)$ are mirror images of one another, which is the dichroic effect. For a fixed CEP and ξ, the angular distributions are highly asymmetric under the transformation $\varphi \to \varphi + \pi$ (or $\hat{\mathbf{p}} \to -\hat{\mathbf{p}}$). In contrast, Fig. 2(c) shows the $L = 1$ part of the TDP, $\mathcal{W}^{(L=1)}(\hat{\mathbf{p}},\mathbf{e})$, which we find is CEP independent and symmetric under the transformation $\varphi \to \varphi + \pi$. This is consistent with first-order PT, in which $\mathcal{W}^{(L=1)} \propto |A_1|^2$ [cf. Eq. (3)]. In the PT limit in which $\mathcal{W}(\hat{\mathbf{p}},\mathbf{e}) \propto |A_1 + A_2|^2$, the difference $\mathcal{W}(\hat{\mathbf{p}},\mathbf{e}) - \mathcal{W}(-\hat{\mathbf{p}},\mathbf{e})$ thus measures directly the cross term $2\mathrm{Re}(A_1^* A_2)$, as in the case of DPI of He by a linearly polarized, few-cycle pulse [29].

The angular dependence of the dichroism $\Delta\mathcal{W}_\xi$ (1) is plotted in Figs. 3(a) and 3(b) for two CEPs; its dependence

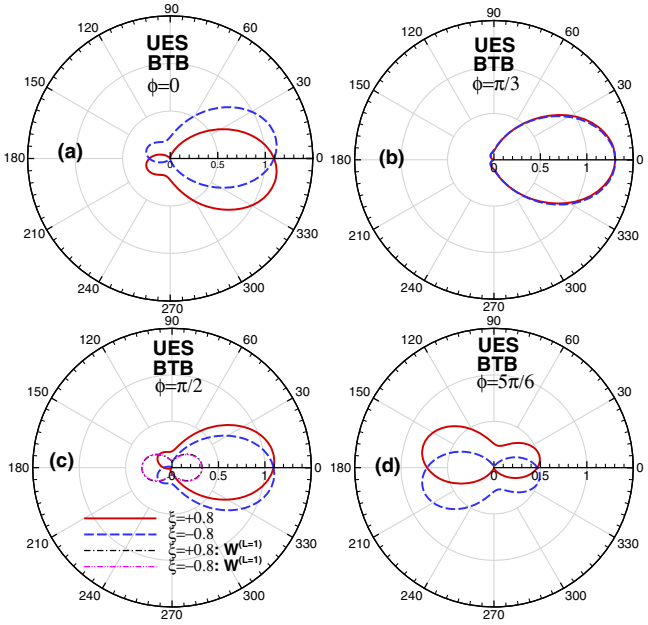

FIG. 2 (color online). The TDP $\mathcal{W}(\hat{\mathbf{p}},\mathbf{e})$ [Eq. (6)] (in units of 10^{-5} a.u.) vs. φ [cf. Fig. 1(b)] for DPI of He by a three-cycle XUV pulse (with $\omega = 65$ eV, $I = 2$ PW/cm^2, $T = 190.9$ as, a $\cos^2$ envelope, and an ellipticity $\eta = \pm 0.5$ or $\xi = \pm 0.8$) for four CEPs: (a) $\phi = 0$, (b) $\phi = \pi/3$, (c) $\phi = \pi/2$, (d) $\phi = 5\pi/6$. All results are for the back-to-back geometry and unequal energy sharing (UES): $E_1 = 0.7$ eV and $E_2 = 3.3$ eV. In (c) we give for comparison $\mathcal{W}^{(L=1)}(\mathbf{p},\mathbf{e})$; see text for discussion.

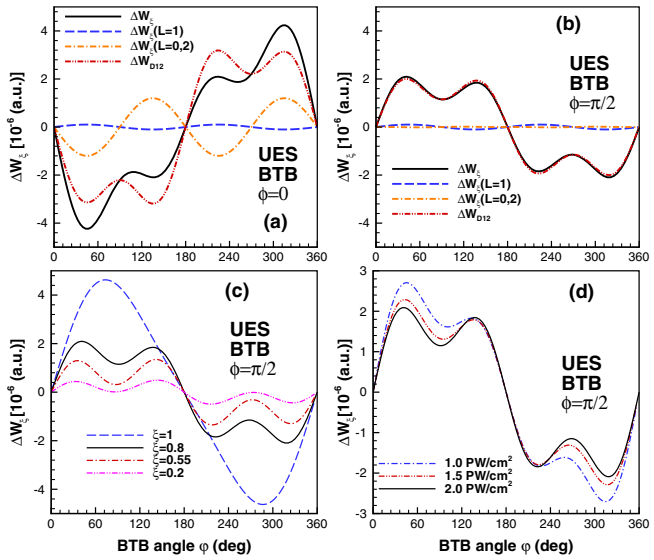

FIG. 3 (color online). Angular dependence of the dichroism, $\Delta\mathcal{W}_\xi$, for two CEPs: (a) $\phi = 0$, and (b) $\pi/2$. The contributions of $\Delta\mathcal{W}_\xi^{(L=1)} \approx \Delta\mathcal{W}_{D1}$, $\Delta\mathcal{W}_\xi^{(L=0,2)} = \Delta\mathcal{W}_{D2}$, and $\Delta\mathcal{W}_{D12}$ are also shown (see text for discussion). (c) Ellipticity dependence of $\Delta\mathcal{W}_\xi$. (d) Pulse intensity-dependence of $\Delta\mathcal{W}_\xi$; results are scaled by $(I/I_r)^{3/2}$, where $I_r = 2$ PW/cm^2. Unless otherwise specified, $\phi = \pi/2$, $\xi = 0.8$, $I = 2$ PW/cm^2, $E_1 = 0.7$ eV, and $E_2 = 3.3$ eV.

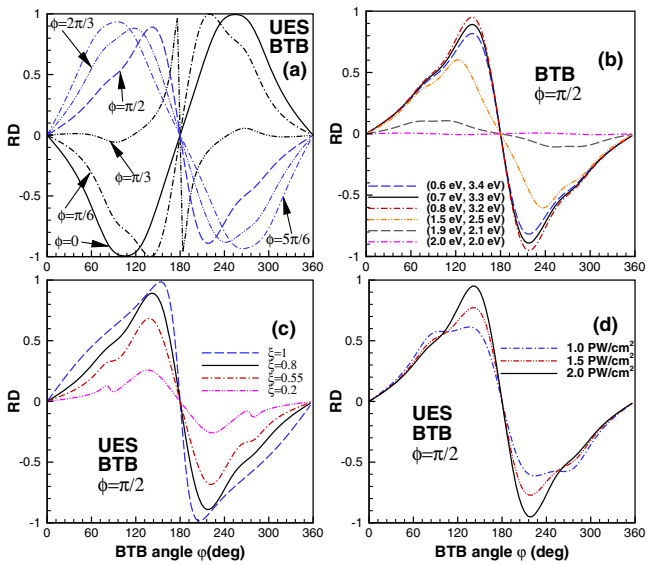

FIG. 4 (color online). Angular dependence of the relative dichroism (RD), $\Delta\mathcal{W}_\xi/[\mathcal{W}(\hat{\mathbf{p}}, \mathbf{e}) + \mathcal{W}(\hat{\mathbf{p}}, \mathbf{e}^*)]$, for the BTB geometry [cf. Fig. 1(b)]. Unless otherwise specified, $\phi = \pi/2$, $\xi = 0.8$, $I = 2$ PW/cm^2, $E_1 = 0.7$ eV, and $E_2 = 3.3$ eV. The panels show its sensitivity to (a) the CEP, (b) the energy sharing, (c) the ellipticity, and (d) the pulse intensity.

on ellipticity and intensity for $\phi = \pi/2$ is shown in Figs. 3(c) and 3(d). One sees that $\Delta\mathcal{W}_\xi$, which includes both the circular dichroism term $\Delta\mathcal{W}_{D1}$ [Eq. (4)] and higher-order dichroism terms [e.g., $\Delta\mathcal{W}_{D12}$ [Eq. (5)] and $\Delta\mathcal{W}_{D2}$], is highly sensitive to the CEP, decreases with decreasing ellipticity, and scales approximately as $I^{3/2}$ with intensity, with deviations originating from higher order terms. To estimate the contributions of each term, we plot in Figs. 3(a) and 3(b) $\Delta\mathcal{W}_\xi^{(L)}$ for the odd and even L components of the two-electron continuum wave packet, where $\Delta\mathcal{W}_\xi^{(L=1)} \approx \Delta\mathcal{W}_{D1}$, $\Delta\mathcal{W}_\xi^{(L=0,2)} = \Delta\mathcal{W}_{D2}$, and thus $\Delta\mathcal{W}_{D12} \approx \Delta\mathcal{W}_\xi - \Delta\mathcal{W}_\xi^{(L=1)} - \Delta\mathcal{W}_\xi^{(L=0,2)}$. We see that $\Delta\mathcal{W}_\xi^{(L=1)}$ is very small, consistent with first-order PT in which $\Delta\mathcal{W}_{D1}$ is zero in the BTB configuration. The nonzero $\Delta\mathcal{W}_\xi^{(L=1)}$ is CEP-independent, as expected for interference between first- and third-order PT amplitudes.

The significance of the second-order dichroism $\Delta\mathcal{W}_{D2}$ term depends on the CEP. For $\phi = \pi/2$ [cf. Fig. 3(b)], $\Delta\mathcal{W}_{D2} \ll \Delta\mathcal{W}_{D12}$ so that $\Delta\mathcal{W}_\xi \approx \Delta\mathcal{W}_{D12}$ at all angles. However, for a CEP $\phi = 0$ [cf. Fig. 3(a)] the magnitude of $\Delta\mathcal{W}_{D2}$ is comparable to that of $\Delta\mathcal{W}_{D12}$, so that $\Delta\mathcal{W}_\xi \approx \Delta\mathcal{W}_{D12} + \Delta\mathcal{W}_{D2}$. Thus for some values of φ, the second-order part of the TDP ($\propto |A_2|^2$) must be included in the PT analysis. Our results in Fig. 3 confirm the PT prediction that $\Delta\mathcal{W}_{D12} \sim \sin\varphi$ [cf. Eq. (5)], i.e., $\Delta\mathcal{W}_{D12} = 0$ when electrons are emitted along the major axis of the pulse polarization ellipse. Figures 3(a) and 3(b) show also that $\Delta\mathcal{W}_{D2} = 0$ for $\varphi = 0, \pi/2, \pi, 3\pi/2$, indicating that $\Delta\mathcal{W}_{D2} \propto \sin\varphi\cos\varphi$, as predicted by PT [34].

In Fig. 4(a) we show that the relative dichroism, $\Delta\mathcal{W}_\xi/[\mathcal{W}(\hat{\mathbf{p}}, \mathbf{e}) + \mathcal{W}(\hat{\mathbf{p}}, \mathbf{e}^*)]$, is sensitive to the CEP and, for nearly all CEPs, is substantial. Its suppression for $\phi = \pi/3$ is consistent with the similarity of the TDPs for $\xi = \pm 0.8$ shown in Fig. 2(b); its large values near $\varphi = \pi$ stem from the small values of the TDPs there. In Figs. 4(b)–4(d), respectively, we see that it decreases as one approaches equal energy sharing and as either the ellipticity or the intensity decrease.

In summary, by solving *ab initio* the six-dimensional two-electron TDSE for DPI of He by an elliptically polarized, intense few-cycle attosecond pulse, we have analyzed the dependence of the TDP on the pulse polarization and CEP. For such few-cycle pulses, a new type of nonlinear (in the field intensity) dichroic effect in the two-electron angular distributions [Eq. (1)] is predicted that can serve as a temporal measure of electron correlations (as it vanishes for long pulses). Our essentially exact numerical results show that, for pulse intensities that may be realized in the near future, PT can be successfully used to predict and explain characteristic features of this new polarization effect, which originates primarily from interference of the first- and second-order PT amplitudes. Our results show that ND is highly sensitive to the pulse CEP. Accordingly, by tuning the CEP one can vary the relative contributions to the total ND of different PT amplitudes, thereby allowing one to determine their relative magnitudes. In the future, ND may be observed experimentally using reaction microscope

techniques [50] with the detection of electrons ionized in opposite directions in the pulse polarization plane for two helicities: $\pm\xi$. We note that linear dichroic effects in He have recently been employed to determine the polarization of an XUV free-electron laser beam [51]. The ND predicted here, owing to its dependence on the large bandwidth of attosecond pulses and its sensitivity to the CEP, may be valuable for characterizing these much shorter pulses.

This work is supported in part by DOE Grant No. DE-FG03-96ER14646, by RFBR Grant No. 13-02-00420, by Ministry of Education and Science of the Russian Federation Project No. 1019, by DOE NNSA Award No. DE-NA0001944, and by ERC-StG Project No. 277767 - TDMET. Our computations use Kraken (NICS) and Stampede (TACC), under Grant No. TG-PHY-120003; and Sandhills, Tusker, and Crane at the Holland Computing Center, University of Nebraska.

[1] J. S. Briggs and V. Schmidt, J. Phys. B **33**, R1 (2000).
[2] H. Hasegawa, E. J. Takahashi, Y. Nabekawa, K. L. Ishikawa, and K. Midorikawa, Phys. Rev. A **71**, 023407 (2005).
[3] A. A. Sorokin, M. Wellhöfer, S. V. Bobashev, K. Tiedtke, and M. Richter, Phys. Rev. A **75**, 051402(R) (2007).
[4] A. Rudenko *et al.*, Phys. Rev. Lett. **101**, 073003 (2008).
[5] M. Kurka *et al.*, New J. Phys. **12**, 073035 (2010).
[6] A. Rudenko *et al.*, J. Phys. B **43**, 194004 (2010).
[7] S. Laulan, H. Bachau, B. Piraux, J. Bauer, and G. L. Kamta, J. Mod. Opt. **50**, 353 (2003).
[8] B. Piraux, J. Bauer, S. Laulan, and H. Bachau, Eur. Phys. J. D **26**, 7 (2003).
[9] S. Laulan and H. Bachau, Phys. Rev. A **68**, 013409 (2003).
[10] S. X. Hu, J. Colgan, and L. A. Collins, J. Phys. B **38**, L35 (2005).
[11] E. Foumouo, G. L. Kamta, G. Edah, and B. Piraux, Phys. Rev. A **74**, 063409 (2006).
[12] E. Foumouo, Ph. Antoine, H. Bachau, and B. Piraux, New J. Phys. **10**, 025017 (2008).
[13] J. Feist, S. Nagele, R. Pazourek, E. Persson, B. I. Schneider, L. A. Collins, and J. Burgdörfer, Phys. Rev. A **77**, 043420 (2008).
[14] X. Guan, K. Bartschat, and B. I. Schneider, Phys. Rev. A **77**, 043421 (2008).
[15] J. Feist, S. Nagele, R. Pazourek, E. Persson, B. I. Schneider, L. A. Collins, and J. Burgdörfer, Phys. Rev. Lett. **103**, 063002 (2009).
[16] A. Palacios, T. N. Rescigno, and C. W. McCurdy, Phys. Rev. Lett. **103**, 253001 (2009).
[17] Z. Zhang, L.-Y. Peng, Q. Gong, and T. Morishita, Opt. Express **18**, 8976 (2010).
[18] E. Foumouo, A. Hamido, Ph. Antoine, B. Piraux, H. Bachau, and R. Shakeshaft, J. Phys. B **43**, 091001 (2010).
[19] A. Palacios, D. A. Horner, T. N. Rescigno, and C. W. McCurdy, J. Phys. B **43**, 194003 (2010).
[20] R. Pazourek, J. Feist, S. Nagele, E. Persson, B. I. Schneider, L. A. Collins, and J. Burgdörfer, Phys. Rev. A **83**, 053418 (2011).
[21] Z. Zhang, L.-Y. Peng, M.-H. Xu, A. F. Starace, T. Morishita, and Q. Gong, Phys. Rev. A **84**, 043409 (2011).
[22] L. Argenti, R. Pazourek, J. Feist, S. Nagele, M. Liertzer, E. Persson, J. Burgdörfer, and E. Lindroth, Phys. Rev. A **87**, 053405 (2013).
[23] W.-C. Jiang, L.-Y. Peng, W.-H. Xiong, and Q. Gong, Phys. Rev. A **88**, 023410 (2013).
[24] C. P. J. Martiny, M. Abu-samha, and L. B. Madsen, J. Phys. B **42**, 161001 (2009).
[25] E. A. Pronin, A. F. Starace, M. V. Frolov, and N. L. Manakov, Phys. Rev. A **80**, 063403 (2009).
[26] C. P. J. Martiny, M. Abu-samha, and L. B. Madsen, Phys. Rev. A **81**, 063418 (2010).
[27] M. Abu-samha and L. B. Madsen, Phys. Rev. A **84**, 023411 (2011).
[28] A. N. Pfeiffer, C. Cirelli, M. Smolarski, D. Dimitrovski, M. Abu-samha, L. B. Madsen, and U. Keller, Nat. Phys. **8**, 76 (2012).
[29] J. M. Ngoko Djiokap, N. L. Manakov, A. V. Meremianin, and A. F. Starace, Phys. Rev. A **88**, 053411 (2013).
[30] L.-Y. Peng, E. A. Pronin, and A. F. Starace, New J. Phys. **10**, 025030 (2008).
[31] J. M. Ngoko Djiokap, S. X. Hu, W.-C. Jiang, L.-Y. Peng, and A. F. Starace, New J. Phys. **14**, 095010 (2012).
[32] J. M. Ngoko Djiokap, S. X. Hu, W.-C. Jiang, L.-Y. Peng, and A. F. Starace, Phys. Rev. A **88**, 011401(R) (2013).
[33] N. L. Manakov, M. V. Frolov, B. Borca, and A. F. Starace, J. Phys. B **36**, R49 (2003), Sec. 1.1.
[34] See Supplemental Material at http://link.aps.org/supplemental/10.1103/PhysRevLett.113.223002 for a more detailed discussion of our PT analysis, including the assumptions leading to Eq. (2), the derivation of Eq. (5), and an explanation of the φ dependence of $\Delta\mathcal{W}_{D2}$ [cf. Fig. 1(b)].
[35] J. Berakdar and H. Klar, Phys. Rev. Lett. **69**, 1175 (1992).
[36] J. Berakdar, H. Klar, A. Huetz, and P. Selles, J. Phys. B **26**, 1463 (1993).
[37] N. L. Manakov, S. I. Marmo, and A. V. Meremianin, J. Phys. B **29**, 2711 (1996).
[38] V. Mergel *et al.*, Phys. Rev. Lett. **80**, 5301 (1998).
[39] A. S. Kheifets and I. Bray, Phys. Rev. Lett. **81**, 4588 (1998).
[40] A. Y. Istomin, N. L. Manakov, and A. F. Starace, Phys. Rev. A **69**, 032713 (2004).
[41] L. Avaldi and A. Huetz, J. Phys. B **38**, S861 (2005).
[42] H. G. Muller, Laser Phys. **9**, 138 (1999).
[43] T. K. Kjeldsen, L. A. A. Nikolopoulos, and L. B. Madsen, Phys. Rev. A **75**, 063427 (2007).
[44] N. I. Shvetsov-Shilovski, D. Dimitrovski, and L. B. Madsen, Phys. Rev. A **87**, 013427 (2013).
[45] S. X. Hu, Phys. Rev. E **81**, 056705 (2010).
[46] L. B. Madsen, L. A. A. Nikolopoulos, T. K. Kjeldsen, and J. Fernández, Phys. Rev. A **76**, 063407 (2007).
[47] G. Sansone *et al.*, Science **314**, 443 (2006).
[48] E. Goulielmakis *et al.*, Science **320**, 1614 (2008).
[49] M. Gailitis, J. Phys. B **23**, 85 (1990).
[50] J. Ullrich, R. Moshammer, A. Dorn, R. Dörner, L. Ph. H. Schmidt, and H. Schmidt-Böcking, Rep. Prog. Phys. **66**, 1463 (2003).
[51] T. Mazza *et al.*, Nat. Commun. **5**, 3648 (2014).